BBA - Biomembranes 1864 (2022) 183819

Contents lists available at ScienceDirect

BBA - Biomembranes

journal homepage: www.elsevier.com/locate/bbamem

Growth-phase dependence of bacterial membrane lipid profile and labeling for in-cell solid-state NMR applications

Florent Laydevant [a], Mahsa Mahabadi [a], Pierre Llido [a], Jean-Philippe Bourgouin [a], Laurence Caron [a], Alexandre A. Arnold [a], Isabelle Marcotte [a,**], Dror E. Warschawski [a,b,*]

[a] Department of Chemistry, Université du Québec à Montréal, C.P. 8888, Succursale Centre-Ville, Montreal H3C 3P8, Canada
[b] Laboratoire des Biomolécules, LBM, CNRS UMR 7203, Sorbonne Université, École normale supérieure, PSL University, 75005 Paris, France

ARTICLE INFO

Keywords:
Escherichia coli
Bacillus subtilis
Bacteria
Phospholipids
Deuterium
GCMS

ABSTRACT

Cell labeling is a preliminary step in multiple biophysical approaches, including the solid-state nuclear magnetic resonance (NMR) study of bacteria *in vivo*. Deuterium solid-state NMR has been used in the past years to probe bacterial membranes and their interactions with antimicrobial peptides, following a standard labeling protocol. Recent results from our laboratory on a slow-growing bacterium has shown the need to optimize this protocol, especially the bacterial growth time before harvest and the concentration of exogenous labeled fatty acids to be used for both *Escherichia coli* and *Bacillus subtilis*. It is also essential for the protocol to remain harmless to cells while providing optimal labeling. We have therefore developed a fast and facile approach to monitor the lipid composition of bacterial membranes under various growth conditions, combining solution ^{31}P NMR and GCMS. Using this approach, the optimized labeling conditions of *Escherichia coli* and *Bacillus subtilis* with deuterated palmitic acid were determined. Our results show a modification of *B. subtilis* phospholipid profile as a function of the growth stage, as opposed to *E. coli*. Our protocol recommends low concentrations of exogenous palmitic acid in the growth medium, and bacteria harvest after the exponential phase.

1. Introduction

For the past four decades, the ^{2}H solid-state Nuclear Magnetic Resonance (SS-NMR) study of living bacteria has intended to better understand bacterial membranes composition, structure, dynamics and interactions with antimicrobial peptides [1–10]. In the seminal work of Davis in 1979, deuterium labeling of *Escherichia coli* membranes was obtained by growing bacteria in the presence of exogenous labeled fatty acids (FAs) at a concentration of 190 μM micellized in Brij® 58, and bacteria were harvested at the mid-log growth phase. Similar parameters were applied by Pius et al. in 2012 [2]. In these works, mutants that cannot synthesize FAs were utilized. In the following years, our group has tested several detergents, and replaced Brij® by either dodecylphosphocholine (DPC) or polyoxyethylene sorbitan monolaurate (also known as Tween® 20) [3,7], and confirmed that non-mutated *E. coli* supplemented with palmitic acid (PA or C16:0) requires an equal amount of oleic acid (OA or C18:1) to maintain the level of unsaturated lipids in the bacterial membranes [5]. More recently, the study of a slow-

Abbreviations: B. subtilis, *Bacillus subtilis* 168; BCFAs, branched chain fatty acids; $CDCl_3$, deuterochloroform; CL, cardiolipin; DCM-MeOH, dichloromethane-methanol; DPC, dodecylphosphocholine; *E. coli*, *Escherichia coli* BL21; EDTA, ethylenediaminetetraacetic free acid; Egg SM, chicken egg sphingomyelin (mostly N-palmitoyl-D-erythro-sphingosylphosphorylcholine); FAs, fatty acids; FAME mix, fatty acid methyl ester mix C4-C24; GCMS, gas chromatography combined with mass spectrometry; LCMS, liquid chromatography combined with mass spectrometry; LPG, lysyl-phosphatidylglycerol; M_2, second spectral moment of ^{2}H SS-NMR spectra; MAS, magic-angle spinning; OA, oleic acid or octadecenoic acid or C18:1; OD_{600}, optical density at 600 nm; PA, palmitic acid or hexadecanoic acid or C16:0; PA-d_{31}, perdeuterated palmitic acid; PE, phosphatidylethanolamine; PG, phosphatidylglycerol; PhA, phosphatidic acid; POPA, 1-palmitoyl-2-oleoyl-sn-glycero-3-phosphate; POPC, 1-palmitoyl-2-oleoyl-glycero-3-phosphocholine; POPE, 1-palmitoyl-2-oleoyl-sn-glycero-3-phosphoethanolamine; POPG, 1-palmitoyl-2-oleoyl-sn-glycero-3-phospho-(1′-rac-glycerol); POPS, 1-palmitoyl-2-oleoyl-sn-glycero-3-phospho-L-serine; PS, phosphatidylserine; SS-NMR, solid-state Nuclear Magnetic Resonance; TMCL, 1′,3′-bis[1,2-dimyristoyl-sn-glycero-3-phospho]-glycerol; TMP, trimethyl phosphate; Tween® 20, polyoxyethylene sorbitan monolaurate; UFAs, unsaturated fatty acids; SFAs, non-branched saturated fatty acids; S/U, saturated/unsaturated.

* Corresponding author at: Laboratoire des Biomolécules, LBM, CNRS UMR 7203, Sorbonne Université, 4 place Jussieu, 75005 Paris, France.
** Corresponding author.
E-mail addresses: marcotte.isabelle@uqam.ca (I. Marcotte), dror.warschawski@sorbonne-universite.fr (D.E. Warschawski).

https://doi.org/10.1016/j.bbamem.2021.183819
Received 1 October 2021; Received in revised form 31 October 2021; Accepted 5 November 2021
Available online 17 November 2021

growing marine bacterium, *Vibrio splendidus*, in presence of exogenous FAs has also shown a change in the acyl chain profile as a function of the growth phase [8]. This observation is not surprising since bacteria are known to adapt very quickly to their environment, and for example to change their membrane properties by adjusting their lipid composition, *i.e.*, both their FAs and headgroup profiles, depending on the growth conditions [11–18]. In humans as well, alteration of lipid homeostasis has been linked to many pathologies, and the increasing number of lipid profile studies has given birth to a new field of research called lipidomics [19].

Based on these observations, and on a growing interest for in-cell biophysical approaches, we have undertaken the optimization of bacterial membrane deuteration, of both the Gram-negative *E. coli* and the Gram-positive *Bacillus subtilis*, focusing on the growth phase at harvest but also on the concentration of exogenous FAs added in the growth medium. Optimization of bacterial labeling aims for the best possible deuteration yield, but also for the least perturbation of bacterial membrane composition and properties, to preserve the native lipid profile and membrane fluidity as much as possible. In order to follow the lipid metabolism in *E. coli* and *B. subtilis*, it is important to characterize the bacterial membranes in a systematic way; therefore, we have optimized a routine protocol to evaluate the lipid composition of bacteria, both their headgroups and FAs, compatible with the high-throughput requirements of growth optimization, implying fast experiments with standard laboratory equipment.

While the determination of the FA profile by gas chromatography combined with mass spectrometry (GCMS) is commonly used to assess cell membrane composition [20,21], headgroup profile investigation has often been neglected, possibly missing out valuable information. The identification of lipid headgroups is usually performed by thin-layer chromatography [22–26], but solution ^{31}P NMR can be used to identify and quantify cell membrane phospholipids, although it has rarely been applied to bacterial samples [27–37]. More recently, liquid chromatography combined with mass spectrometry (LCMS) provided a much more powerful approach [38–43], allowing to determine both headgroup and FA composition with very high sensitivity and resolution. Nevertheless, LCMS instruments dedicated to lipid analysis are rare and the experiments are costly. In short, there is no perfect routine protocol currently available to rapidly assess changes in the lipid headgroup and FA chain composition.

The main advantage of the protocol we present here is that it is fast, providing results in less than 24 h, with several samples possibly running in parallel. In addition, it only requires GCMS and NMR equipment found in standard chemistry or biochemistry laboratories or departments. In the context of lipidomics, this protocol may become handy for a fast and facile phospholipid profile determination. It allowed us to optimize *E. coli* and *B. subtilis* membrane isotopic labeling, by reducing the amount of exogenous FAs initially recommended by Davis [1], by comparing the efficiency of several detergents, and by selecting the appropriate harvest time for NMR experiments to be reproducible and have a high signal-to-noise ratio. This robust protocol has provided us with ideal labeling conditions, but also a complete lipid profile and membrane lipid order assessment of *E. coli* and *B. subtilis* membranes that will serve as a standard for future studies.

2. Experimental section

2.1. Materials

Palmitic acid (hexadecanoic acid), oleic acid (octadecenoic acid), fatty acid methyl ester mix C4-C24 (FAME mix), guanidinium hydrochloride, deuterium-depleted water, trimethyl phosphate (TMP) and HPLC-grade organic solvents were purchased from Sigma-Aldrich (St. Louis, MO, USA) while ethylenediaminetetraacetic free acid (EDTA) was purchased from Fisher Scientific (Fair Lawn, NJ, USA). Perdeuterated palmitic acid (PA-d_{31}) and deuterochloroform ($CDCl_3$) were obtained from Cambridge Isotope Laboratories (Tewksbury, MA, USA). Dodecylphosphocholine (DPC) was purchased from Anatrace Products (Maumee, OH, USA), and polyoxyethylene sorbitan monolaurate (Tween® 20) was bought from BioShop (Burlington, ON, Canada). Synthetic lipids 1-palmitoyl-2-oleoyl-sn-glycero-3-phosphoethanolamine (POPE), 1-palmitoyl-2-oleoyl-sn-glycero-3-phospho-(1′-rac-glycerol) (POPG), 1′,3′-bis[1,2-dimyristoyl-sn-glycero-3-phospho]-glycerol (TMCL), 1-palmitoyl-2-oleoyl-glycero-3-phosphocholine (POPC), 1-palmitoyl-2-oleoyl-sn-glycero-3-phospho-L-serine (POPS), 1-palmitoyl-2-oleoyl-sn-glycero-3-phosphate (POPA), and chicken egg sphingomyelin (mostly N-palmitoyl-D-erythro-sphingosylphosphorylcholine, or Egg SM) were purchased from Avanti Polar Lipids (Alabaster, AL, USA). *Escherichia coli* BL21 (*E. coli*) was kindly provided by Pr. Catherine Paradis-Bleau from the Université de Montréal (Canada), and *Bacillus subtilis* 168 (*B. subtilis*) was obtained from the Bacillus Genetic Stock Center at Ohio State University (USA). All experiments were performed at least in triplicates.

2.2. Bacterial growth

Both *E. coli* and *B. subtilis* strains were grown at 37 °C on a shaker (220 rpm) in Luria Broth (LB) medium containing 10 g/L peptone, 10 g/L NaCl, and 5 g/L yeast in deionized water at pH 7.2. When necessary, exogenous FAs were solubilized in appropriate quantities for the final culture volume with either DPC (final concentration 1 mM) or Tween® 20 (final concentration 0.15 mM) in 15 mL of LB medium, by four alternating series of freeze (liquid N_2)/thaw (95 °C)/vortex shaking cycles, until the palmitic acid crystals had melted. This solution was then added, while still hot, to the culture medium. The bacterial cultures (usually 300 mL) were stopped either at mid-log (optical density at 600 nm (OD_{600}) around 1.5, after approximately 2.5 h for *E. coli* and 3.5 h for *B. subtilis*), or at the early stationary phase ($OD_{600} \sim 3$, after approximately 5.5 h for *E. coli* and 6 h for *B. subtilis*), and centrifuged at 3000*g* for 10 min to collect the pellets, either for ^{2}H SS-NMR or for lipid profile determination. For ^{2}H SS-NMR, the pellet was washed with 0.85% NaCl solution in deionized water once, then once with 1 mL of 0.85% NaCl solution in ^{2}H-depleted water, transferred to a 4-mm NMR rotor, and used as soon as possible. For lipid profile determination, the pellet was washed with deionized water, centrifuged, freeze-dried and stored at −20 °C. For 300 mL of culture, 100–200 mg of wet pellets could be obtained, corresponding to 50–100 mg of dry pellets, depending on the strain and the growth time.

2.3. Lipid extraction

Cell pellets from *B. subtilis* and *E. coli* grown with or without exogenous FAs were extracted by the Folch method [44]. In short, each pellet was solubilized in about 30 mL of 2:1 dichloromethane-methanol (DCM-MeOH), then sonicated for about 10 min at 8 W on ice (by alternating 1 min sonication and 1 min sample rest, five times), and transferred to a separating funnel. Then 70 mL of DCM:MeOH (2:1) and 27 mL of KCl aqueous solution (0.88% *w/v*) were added. After shaking, two phases were separated in about 20 min. The lower organic phase was collected, filtered through Whatman grade 54 filter paper, dried with a rotary evaporator, and freeze-dried for an extra hour. The mass of dry lipids obtained after this procedure was around 3 to 6 mg and, if necessary, lipids were kept at −80 °C.

2.4. Lipid hydrolysis and fatty acid methylation

After the solution NMR experiments, the lipid solution was retrieved from the NMR tube, dried under a nitrogen gas flow and heated at 40 °C. Lipids were then hydrolysed and FAs methylated for GCMS analysis in one step by a standard method described previously [3]. In short, FAs were resuspended in 2 mL of H_2SO_4 (2% in MeOH) and 800 μL of toluene, and heated in a sealed vial for 10 min at 100 °C. After cooling

for 10 min, 4 mL of H_2O and 800 μL of hexane were added, the vial was vortexed and left to stand until two phases separated. The upper organic phase containing the FAMEs was dried under nitrogen gas at room temperature to preserve the short FAs. The mass of dry FAMEs obtained after this procedure was around 2 to 4 mg. Before GCMS analysis, dry FAMEs were resuspended in hexane at an approximate concentration of 1 mg/mL. The standard FAME mix was also resuspended in hexane at a concentration of 1 mg/mL.

2.5. ^{31}P solution NMR

Phospholipids were identified and quantified by ^{31}P solution NMR by solubilizing dry lipids in an organic solvent solution, placing it in a standard 5-mm solution NMR tube. Two solutions were compared: the biphasic solution composed of 500 μL of $CDCl_3$, 200 μL of MeOH, and 50 μL of aqueous EDTA solution [27,29,31,32], and the *CUBO* solution, made of 500 μL of dimethylformamide, 150 μL of triethylamine, and 50 mg of guanidinium hydrochloride [28,30,35]. Note that in the *CUBO* solution, there is no deuterated compound for locking or shimming. Following Murgia et al. [30], we referenced our spectra with internal trimethyl phosphate (TMP) at 1 mM, which is soluble both in $CDCl_3$ and dimethylformamide. TMP ^{31}P chemical shift in the biphasic solution is 2.01 ppm, while it is 2.42 ppm in the *CUBO* solution. The aqueous EDTA solution (200 mM at pH 6) was prepared with EDTA free acid and slowly adding KOH to reach pH 6, without crossing this value.

Solution NMR spectra were recorded on a Bruker Avance III-HD 600 spectrometer (Milton, ON, Canada), operating at a frequency of 242.84 MHz for ^{31}P and 599.95 MHz for ^{1}H, and equipped with a 5-mm BBFO double-resonance probe. For quantitative results, ^{31}P spectra were recorded with a 10 s recycle delay, ^{1}H inverse gated decoupling, and without NOE enhancement. Typically, spectra were acquired at 25 °C, with 128 scans, and a spectral width of 50 ppm, for about 20 min. Each resonance was integrated with the Bruker TopSpin 3.5 software, and areas were corrected to take into account that cardiolipin has two ^{31}P nuclei while other phospholipids have only one. The standard deviation on resulting lipid proportions are indicated, and fall below 10% of the average value.

2.6. ^{2}H solid-state NMR

SS-NMR spectra were recorded on a Bruker Avance III-HD 400 wide bore spectrometer (Milton, ON, Canada), operating at a frequency of 61.4 MHz for ^{2}H, and equipped with a 4-mm magic-angle spinning (MAS) double-resonance probe. Rotors were spun at the magic angle at a spinning frequency of 10 kHz. ^{2}H spectra were recorded at 37 °C with a Hahn echo sequence using a 100 μs delay (one rotor period) and 1 s recycle delay. A typical spectrum was acquired with 3k to 10k scans, and a spectral width of 1 MHz, for about 1 to 3 h. A 100 Hz exponential multiplication was used and spectral moments determined as described by Warnet et al. [5].

2.7. GCMS

GCMS analyses were performed using a GC 7890A chromatograph (Agilent Technologies, Santa Clara, CA, USA) equipped with an HP-5 ms GC column (5% phenyl-methylpolysiloxane) of 30 m length, 0.25-mm inner diameter and 0.25-μm film thickness, and a CombiPAL automated sample injector. The Mass Selective Detector 5975 was used in Electron Impact (EI) mode. Data acquisition and analysis were done with the ChemStation software. A better and faster separation between FAs could be obtained with a 50% cyanopropyl-methylpolysiloxane column, but it was not necessary here.

The carrier gas was helium at a constant flow of 0.52 mL/min. The injection of 1 μL of sample was made in a split mode (50:1) with the injector temperature at 250 °C. The column program was as follows: the initial temperature of 140 °C was held for 5 min, then the temperature was ramped at a rate of 4 °C/min to 300 °C. The source temperature was kept at 230 °C, and the transfer line at 280 °C. EI mode was performed at 70 eV. Full-scan type detection was employed in positive mode on an *m/z* interval of 40–600. Total run time was around 40 min.

Peaks were identified by comparing their retention time to that of the standard FAME mix, and by their mass. The area of each peak was converted into percentage by comparing them to those of the FAME mix. For FAs absent from the FAME mix (cyclopropane, branched or deuterated for example), protonated FAs with the same number of carbons were used. The standard deviations on resulting FA proportions are indicated in Tables 1 and 2, and are all below 10% of the indicated average value for the major species.

3. Results and discussion

3.1. Native E. coli and lipid profile determination

Bacterial cultures were monitored by measuring the OD_{600} every 30 min, and the stationary phase was reached after approximately 5.5 h for *E. coli*. A total of 300 to 500 mL of *E. coli* cultures were then prepared and harvested after either 2.5 h to reach the "mid-log" phase (OD_{600} of 1.5), or 5.5 h to reach the "early stationary" phase (OD_{600} of ~3). Pellets were washed, freeze-dried and stored at −20 °C until their lipid profile was assessed.

A quasi-complete lipid profile could then be determined in less than 24 h. Indeed, the lipid extraction (see Section 2.3) can be performed the first morning in less than 2 h, then the lipids are brought to the NMR facility. Each NMR spectrum acquisition lasts 20 min, and several runs can be performed before lipids are prepared for GCMS. Hydrolysis followed by methylation can be achieved in less than an hour before chromatography. Finally, GCMS is the longest experiment, taking close to 1 h per sample, and is therefore usually carried out overnight as several samples can be analyzed using an auto-sampler, and the results obtained the following morning.

An advantage of NMR for the identification of lipids is that it is a non-destructive method that does not require chemical derivatization; lipids can therefore be recovered intact and further studied. Several solvent mixtures [27–35] or even detergent aqueous solutions such as cholate micelles [36–37] have been suggested in the literature to study lipids by solution NMR. Despite their interesting properties, detergent micelles have been discarded here because, in order to use the same lipid samples for GCMS, molecules that could be confused with a FA were avoided. After trying several options, we adopted the conditions proposed by Flieger et al. [29], which consist in solubilizing the dry lipids in the "biphasic solution" composed of 500 μL of $CDCl_3$, 200 μL of MeOH, and 50 μL of aqueous EDTA solution (200 mM at pH 6). When necessary, the volume of EDTA solution was increased up to 100 μL, and a slight narrowing and shifting of resonances was observed. Although the separation, identification and quantification of the various ^{31}P NMR lipid headgroup resonances in the lipid samples is straightforward, their linewidths and chemical shifts may slightly vary depending on lipid acyl chains, solvent concentration, temperature and the lipids-to-EDTA molar ratio. For those reasons, it is hard to provide precise and reproducible chemical shifts for each lipid and we estimate the precision of the values to be ±0.05 ppm.

Since there is no consensus for lipid ^{31}P NMR chemical shifts in organic solvents, and following Murgia et al. [30], we have also solubilized the dry lipids in the *CUBO* solution, and included trimethyl phosphate (TMP) at 1 mM in some samples for internal ^{31}P reference. The chemicals shifts of TMP at 25 °C are 3.01 ppm in D_2O [45], 2.01 ppm in the biphasic solution, 2.42 ppm in the *CUBO* solution, and 2.53 ppm as a neat liquid. Before analyzing the bacterial lipid pellets, we have assigned the ^{31}P chemical shifts of several synthetic lipids in both solutions (see Table S1). In *E. coli*, we could clearly identify phosphatidylglycerol (PG) at 0.65 ppm, cardiolipin (CL) at *ca.* 0.38 ppm, and phosphatidylethanolamine (PE) at ~0.11 ppm in the biphasic solution,

Table 1
Phospholipid headgroup profile and proportions of saturated fatty acids (SFAs) of *E. coli* respectively, determined by ^{31}P NMR and GCMS (see Table S3), as well as ^{2}H SS-NMR second spectral moment (M_2) under MAS reflecting membrane lipid order. Values (with standard deviation) are reported as a function of added PA-d_{31} and OA for bacteria harvested at different growth stages (mid-log and early stationary). ^{31}P NMR and GCMS analyses were performed in triplicates, with three independent bacterial cultures for each condition. ^{2}H SS-NMR experiments were repeated six times, with six independent bacterial cultures.

	0 μM		50 μM		100 μM		190 μM	
	Mid-log	Early-stat.	Mid-log	Early-stat.	Mid-log	Early-stat.	Mid-log	Early-stat.
PG	19.9% (0.2)	25.8% (0.6)	19.0% (3.2)	23.3% (1.5)	23.1% (1.9)	24.8% 0.8)	22.3% (1.2)	23.5% (0.5)
CL	1.8% (0.3)	1.4% (0.4)	2.7% (0.9)	1.0% (0.3)	1.3% (0.3)	1.3% (0.1)	1.8% (0.5)	2.2% (0.4)
PE	76.9% (2.6)	72.8% (1.0)	78.3% (2.7)	75.7% (1.8)	75.5% (2.2)	73.8% (0.9)	76.0% (1.3)	74.3% (0.1)
SFA	45%	50%	46%	40%	47%	44%	51%	40%
M_2 (10^9 s^{-2})	–	–	1.90 (0.37)	2.02 (0.14)	1.89 (0.62)	2.19 (0.12)	6.87 (5.00)	2.06 (0.6)

Table 2
Phospholipid headgroup profile and proportions of non-branched saturated fatty acids (SFAs) of *B. subtilis* respectively determined by ^{31}P NMR and GCMS (see Table S4), as well as ^{2}H SS-NMR second spectral moment (M_2) reflecting membrane lipid order. Values (with standard deviation) are reported as a function of added PA-d_{31}, for bacteria harvested at different growth stages (mid-log and early stationary). All experiments were performed in triplicates, with three independent bacterial cultures for each condition.

	0 μM		20 μM		50 μM		100 μM		190 μM	
	Mid-log	Early-stat.	Mid-log	Early-stat.	Mid-log	Early-stat.	Mid-log	Early-stat.	Mid-log	Early-stat.
PG	36.5% (2.7)	59.9% (1.0)	36.1% (1.4)	57.8% (4.3)	32.9% (2.2)	44.7% (5.2)	36.1% (3.7)	43.6% (7.4)	29.4% (6.4)	42.8% (2.8)
CL	21.2% (1.8)	8.9% (2.2)	24.9% (1.7)	11.0% (6.2)	27.2% (2.9)	21.3% (4.5)	29.1% (4.8)	27.1% (12.5)	27.8% (5.0)	25.9% (1.0)
PE	33.8% (0.7)	21.1% (3.0)	29.5% (0.5)	21.3% (1.1)	28.9% (1.1)	24.5% (1.9)	27.5% (1.0)	19.1% (3.9)	32.2% (2.2)	20.5% (3.3)
LPG	8.5% (1.5)	10.0% (0.5)	9.5% (0.3)	9.8% (3.7)	11.0% (1.1)	9.5% (2.3)	7.9% (0.8)	10.2% (2.3)	10.7% (2.9)	10.8% (0.4)
SFA	8%	6%	32%	31%	72%	55%	73%	82%	96%	77%
M_2 (10^9 s^{-2})			1.4 (0.1)	1.9 (0.6)	3.4 (0.6)	2.5 (0.7)	19 (10.9)	35 (5.5)	44 (3.2)	27 (15.9)

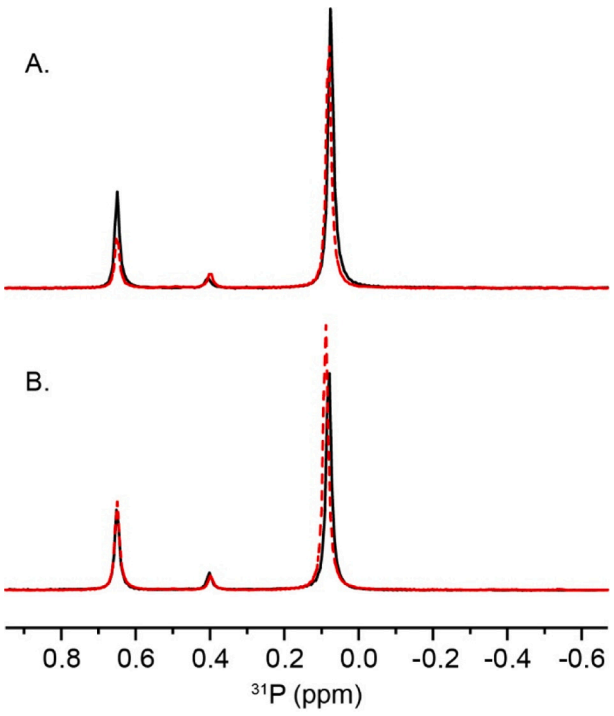

Fig. 1. ^{31}P solution NMR spectra of lipids extracted from *E. coli* harvested at (A) mid-log or (B) early stationary stages, in 500 μL of $CDCl_3$, 200 μL of methanol, and 50 μL of aqueous EDTA solution (200 mM at pH 6). Black: control; Dotted red: *E. coli* grown with 190 μM of PA-d_{31} and OA.

as shown in Fig. 1. Those three peaks appear at 0.77 ppm; 0.25 ppm and 0.05 ppm in the *CUBO* solution (see Fig. S1). The *CUBO* solution can be very useful in case of ambiguous assignments (*vide infra*), but generally speaking the biphasic solution is much more practical since deuterated chloroform enables locking and shimming, which therefore leads to narrower lines. More importantly, as explained by Murgia et al. [30], triethylamine in *CUBO* forms adducts that generate extra resonances for PE at *ca.* −0.31 ppm, and for TMP at *ca.* 1.92 ppm, as well as for phosphatidylserine (PS, see Table S1). The lipid structures are presented in Fig. S2 and the chemical shifts are summarized in Table S2.

Resonances were integrated and the resulting lipid proportions are reported in Table 1. The values obtained in our study are similar to those found in the literature [24], with PE dominating in *E. coli* membranes with a proportion of approximately 75%, followed by PG (~23%), and CL being a minor lipid (1% to 2%).

After lipid hydrolysis and methylation, the FA profile of those bacterial membranes was obtained by GCMS. Values are summarized in Fig. 2 and Table S3, and in agreement with other values reported in the literature [5,20]. The major FAs are the saturated C16:0 (PA), the monounsaturated C18:1 (OA) and the cyclopropane FAs cyC17:0 and, to a lesser extent, cyC19:0, for a total of about 55% unsaturated fatty acids (UFAs) (represented in Fig. S3). With increasing growth time, the proportion of both cyclopropane FAs increased, at the expense of C18:1. The protocol we present here allows for the precise quantification of both the headgroups and FA chains but, as most protocols, it misses the correlation between the two. In other words, the total amount of each lipid class and of each FA is determined, but not the occurrence of each FA *for* each lipid class.

3.2. *E. coli grown with exogenous fatty acids*

To optimize the labeling of *E. coli*, we assessed the lipid profiles of *E. coli* membranes grown in the presence of various concentrations of

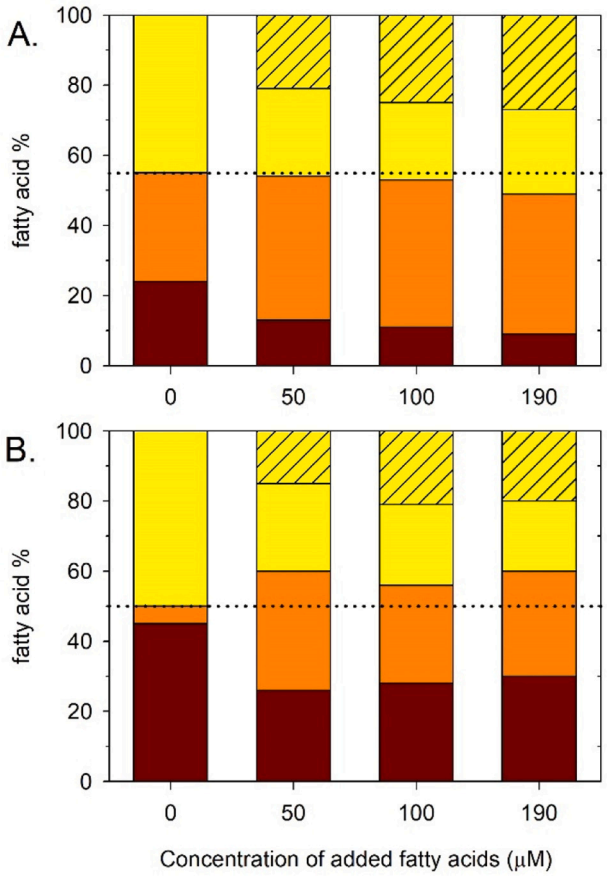

Fig. 2. Fatty acid chain profile in *E. coli* harvested at (A) mid-log and (B) early stationary phases, as a function of the concentration of added PA-d_{31} and OA (in μM) in the growth medium. The percentage of cyclopropane (red), unsaturated (orange) and saturated fatty acids (yellow) were determined by GCMS (see Table S3). The percentage of saturated C16:0 *deuterated* fatty acids is cross hatched. The molar ratio of [saturated]-to-[cyclopropane and unsaturated] fatty acids in the control experiment is indicated by the dotted horizontal line.

exogenous PA and OA (50 μM, 100 μM, 190 μM) micellized with DPC, harvested either at the mid-log or early stationary phases. These profiles are meant to determine the best conditions for *in vivo* ^{2}H SS-NMR analyses, which should preserve the "native" lipid profile, or at least the ratio of saturated/unsaturated (S/U) FAs and membrane fluidity. In addition, since the NMR signal comes from the deuterated PA chains in the lipid membranes, a sufficient amount of labeling has to be reached. Phosphorous-31 solution NMR results are presented in Fig. 1, where lipid ^{31}P chemical shifts and relative proportions are hardly affected by the presence of exogenous FAs (Fig. 2 and Table 1).

Previous experiments had shown that incorporating OA in addition to PA was necessary to maintain the level of UFAs at mid-log phase [5], although the result still differed from the native conditions. However, GCMS results shown here reveal that the UFA level is closer to the control at the early stationary stage (Fig. 2 and Table 1), consistent with the results obtained with the marine Gram(−) bacterium *V. splendidus* [8]. In addition, this holds true when the concentration of added FAs is reduced from 190 μM to 100 μM or even 50 μM (Fig. 2). As expected, the addition of exogenous PA and OA increases the total level of PA and OA in *E. coli*. Here again, measured values are closer to the control at the early stationary stage as compared to mid-log. We hypothesize that the increase in OA chains compensates the decrease in cyclopropane FAs to maintain the fluidity of bacterial membranes. It is worth noticing that the level of cyclopropane FAs, while still low, increases at the early stationary stage (Fig. 2).

The total measured level of PA is divided between natural abundance PA and deuterated PA, and the percentage of deuteration does not seem to be affected by the growth stage (Fig. 2 and Table S3). The labeling is higher in the mid-log phase than in the early stationary phase, and is obviously greater when more exogenous PA-d_{31} is incorporated. The deuteration percentage is still high (above 20%) at 100 μM, and only drops at 50 μM of PA-d_{31}. Finally, while C14:0 is a relatively minor FA (less than 4%), it is noteworthy that deuterated C14:0 FAs were detected in the early stationary phase, indicating that exogenous deuterated C16:0 could be used in the biosynthesis of C14:0 FA phospholipid chains. While this is a known process (β-oxydation), and that it only affects *ca.* 1% of the measured FAs, it is interesting to show that our protocol can reveal such phenomenon, and to observe that there are no other spurious deuterated FAs.

Labeling bacterial membranes with deuterated FAs enables their *in vivo* study by SS-NMR, to probe their structure, dynamics, and altogether general state, as previously shown by us and other groups [1–10]. It also allows assessing the membrane lipid order by monitoring the order parameter of deuterated lipid FA chains. This can be done by measuring the second spectral moment (M_2) of ^{2}H SS-NMR spectra on static samples [1–3,9]. In biological membranes, such measurements can be long compared to the survival time of bacteria, thus we recently introduced a new, more sensitive, and thereby faster way to evaluate M_2. To do so, ^{2}H SS-NMR experiments are carried out under MAS of the sample, thus reducing the total experiment time to an hour [5,6,8,10]. Here, we have used this approach to probe the lipid chain ordering of the same bacteria samples that were studied by GCMS.

Representative spectra are shown in Fig. 3, and extracted M_2 values are reported in Table 1. ^{2}H SS-NMR confirms the GCMS results, *i.e.*, the

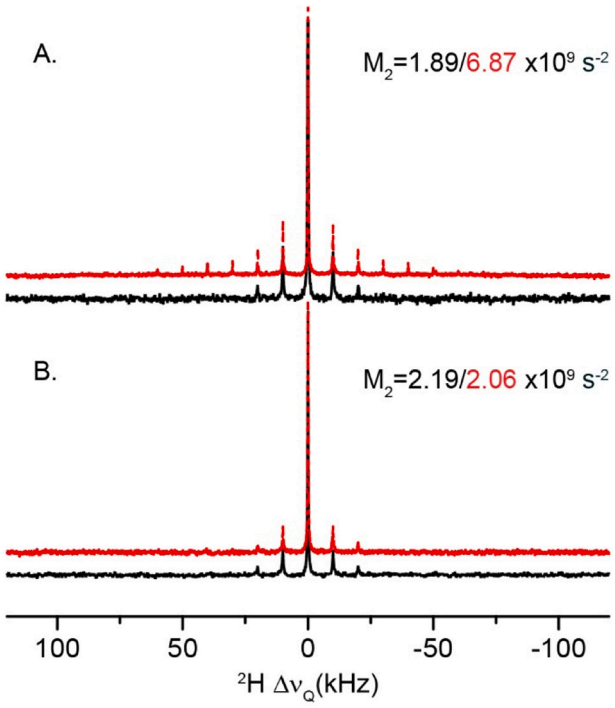

Fig. 3. ^{2}H SS-NMR spectra of *E. coli* spun at 10 kHz and 37 °C. Bacteria were grown with either 100 μM of PA-d_{31} and OA (black) or 190 μM of PA-d_{31} and OA (dotted red) and collected at (A) mid-log or (B) early stationary stages. The resulting M_2 values for all labeling conditions are reported in Table 1. All spectra were normalized with respect to the first spinning sideband to better highlight the sideband intensity distribution. Note that the spectra are zoomed in order to show the difference in sideband intensities, the central peak is thus truncated.

inverse variation of OA and cyclopropane FAs helps maintaining the membrane fluidity. An M_2 value close to 2×10^9 s^{-2} is common in fluid bacterial membranes [5], and the only measured value that is significantly different is the one at mid-log, for 190 μM of exogenous FAs (around 7×10^9 s^{-2}). This condition shows an increased M_2, indicating a more rigid membrane consistent with being the only case where SFAs exceed UFAs (see Table 1). Another striking difference for this condition is the larger standard deviation, calculated for six different experiments. Actual values were measured between 2×10^9 s^{-2} (fluid phase) and 12×10^9 s^{-2} (gel phase), indicating not only that membranes are generally more rigid in this situation, but also that this is an *unstable* growth stage, where little variations can have a strong effect.

Although samples are brought to the NMR spectrometer as soon as the bacterial growth is stopped, the two washing steps and the transfer to the rotor can take between 30 and 60 min, during which bacteria are still alive and continue to grow and metabolize FAs, which could explain the observed variability. To test this hypothesis, we took a sample where at mid-log, for 190 μM of exogenous FAs, a rigid M_2 value of 9.3×10^9 s^{-2} was obtained. The rotor was left for two more hours at 37 °C and the ^{2}H SS-NMR measurement was repeated. Consequently, the M_2 value dropped to 2.6×10^9 s^{-2} (see Fig. S4). Conversely, at the early stationary stage, repeating the experiment 2 h apart provided the same value of M_2. This confirms that short measurements are essential, but also that the mid-log stage is an unstable stage where reproducibility is difficult to obtain.

In summary, our results indicate that optimal *E. coli* labeling is achieved using a total concentration of 100 μM of exogenous PA-d_{31} and OA (1:1) micellized in DPC in the growth medium, and that bacteria should by collected at the early stationary phase. This ensures that over 20% of FAs are deuterated while only the proportion of cyclopropane cyC17:0 FAs is significantly reduced (by a factor of two approximately), compensated by the increase in C18:1 by a similar factor. This also provides a native-like S/U FA ratio and membrane lipid order, as determined by ^{2}H SS-NMR. Similarly, in such conditions, the headgroup profile of *E. coli* is only mildly affected. Last but not least, we have shown that these conditions are also more reproducible than in the mid-log phase where little experimental variations can have strong effects.

3.3. Native Bacillus subtilis and lipid profile determination

B. subtilis cultures were monitored by measuring the OD_{600} every 30 min, and the stationary phase was reached after approximately 6 h for this bacterium. A total of 300 mL of *B. subtilis* cultures were thus grown and harvested after either 3.5 h ("mid-log", OD_{600} of 1.5), or 6 h ("early stationary", OD_{600} of ~3). Pellets were washed, freeze-dried and stored at −20 °C until their lipid profile was assessed. Using the same protocol as the one described for *E. coli*, a quasi-complete lipid profile could then be determined in less than 24 h.

In addition to the same three phospholipid resonances observed with *E. coli*, ^{31}P solution NMR of *B. subtilis* lipids revealed the presence of two more ^{31}P resonances. While we can clearly identify PG at 0.65 ppm, CL at *ca.* 0.37 ppm, and PE at ~0.14 ppm in the biphasic solution, as shown in Fig. 4, we can also observe a fourth peak at −0.11 ppm, as well as a very small peak at −0.48 ppm. Although some authors have suggested that the fourth lipid could be phosphatidylserine (PS) or phosphatidic acid (PhA) identified by thin-layer chromatography [25], the most common hypothesis is that this lipid is lysyl-phosphatidylglycerol (LPG), as suggested by mass spectrometry [39]. To ascertain the nature of this lipid, we have solubilized the dry lipid pellet in a *CUBO* solution and found PG at 0.78 ppm, CL at ~0.25 ppm, PE at ~0.06 ppm (and −0.30 ppm), the fourth lipid at around 0.38 ppm, and the very small peak at −0.08 ppm (see Fig. S1). Based on our measurement (see Table S1) and comparison to published values [30,31], the fourth lipid cannot be ascribed to PhA or PS, but it is compatible with being lysyl-phosphatidylglycerol. We therefore assign this fourth lipid in *B. subtilis* to LPG, which has a chemical shift of −0.11 ppm in the biphasic solution, and of 0.38 ppm in the *CUBO* solution (lipid structures are shown in Fig. S2 and chemical shifts are summarized in Table S2).

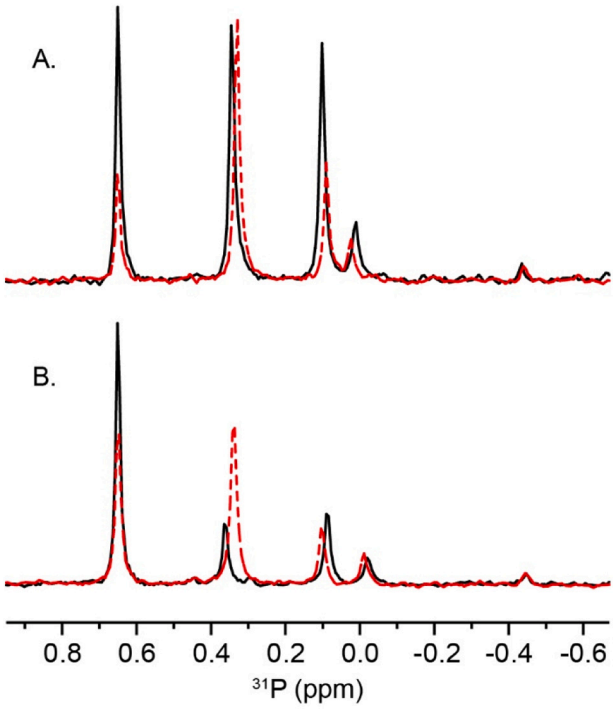

Fig. 4. ^{31}P solution NMR spectra of lipids from *B. subtilis* extracted at (A) mid-log or (B) early stationary stages, in 500 μL of $CDCl_3$, 200 μL of MeOH, and 50 μL of aqueous EDTA solution (200 mM at pH 6). Black: control; Dotted red: *B. subtilis* grown with 190 μM of PA.

Resonances were integrated, and the resulting lipid proportions listed in Table 2 are very variable depending on the growth stage, but are compatible with other values reported in the literature [22,39], with PG dominating (especially at the end of the exponential phase), followed by PE and CL, and LPG being the fourth minor lipid, with a stable proportion of *ca.* ~10%. The very small resonance at −0.48 ppm in the biphasic solution (and −0.08 ppm in the *CUBO* solution) is present on *B. subtilis* spectra but not on *E. coli* spectra. It represents less than 3% of the total lipid phosphorous, and has not been assigned yet.

After hydrolysis and methylation, GCMS provided the FA lipid profile of those bacterial membranes (see Fig. 5 and Table S4 for the full quantification), which is in agreement with other values found in the literature [25,39]. While the major FAs are the branched ones (BCFAs) C15 and C17, with a predominance of the anteiso form, there are few non-branched SFAs and no UFAs (structures are presented in Fig. S3). A similar trend is observed with increasing growth time, except that the proportion of C15 surpasses that of C17.

3.4. B. subtilis grown with exogenous fatty acids

For SS-NMR studies using deuterated PA chains as a probe, our previously published work showed that adding OA was unnecessary for *B. subtilis* [6], and the FA profile determined here confirms that the bacterial membrane does not contain a significant proportion of UFAs. Branched FAs are, on the other hand, abundant, but they are not available commercially at an affordable price. The approach we follow here is to adapt the protocol of Davis [1] by using non-mutated bacteria and optimizing the amount of exogenous PA employed in order to modify as little as possible the "native" lipid profile, while at the same time aiming for the best labeling yield. To do so, we assessed the membrane lipid profile of *B. subtilis* grown either at mid-log or at the

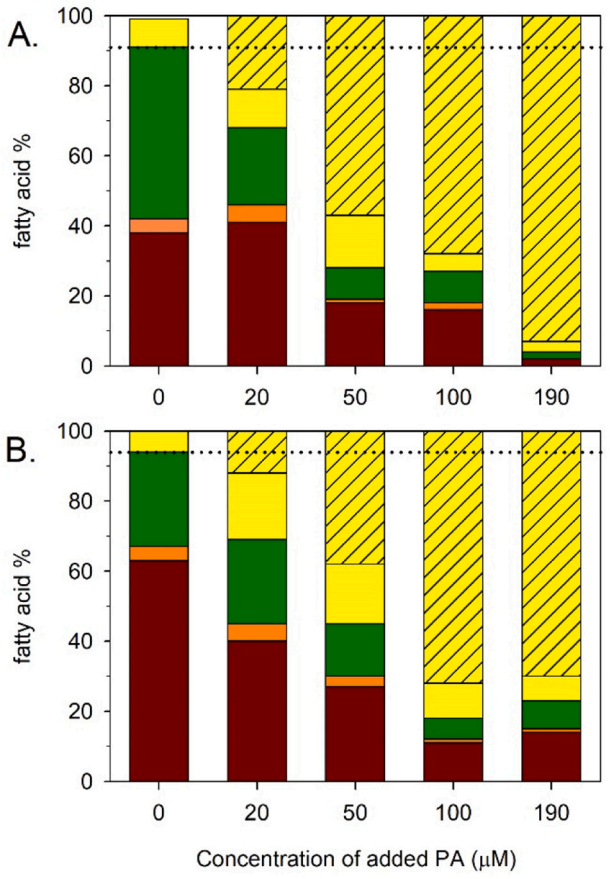

Fig. 5. Fatty acid chain profile in *B. subtilis* harvested at (A) mid-log and (B) early stationary phases, as a function of the concentration of added PA-d_{31} (in μM) in the growth medium. The percentage of branched C15 (red), branched C16 (orange), branched C17 (green) and non-branched (yellow) FAs were determined by GCMS (see Table S4). The percentage of non-branched C16:0 *deuterated* fatty acids is cross hatched. The molar ratio of [branched]-to-[non-branched] fatty acids in the control experiment is indicated by the dotted horizontal line.

early stationary phases, and in presence of exogenous PA-d_{31} (solubilized with Tween® 20) at various concentrations, *i.e.*, 20 μM, 50 μM, 100 μM, 190 μM.

Phospholipids were identified according to their headgroups by ^{31}P solution NMR, and representative spectra are shown in Fig. 4. Resonances were integrated and the resulting lipid proportions are reported in Table 2. As opposed to *E. coli*, the proportion of phospholipids is greatly affected by addition of PA in the growth medium, especially when *B. subtilis* are harvested at the early stationary phase. As can be seen in Table 2, the amount of CL increases at the expense of PG, which is a manifestation of bacterial stress, as previously observed in various contexts [11,15].

FAs were identified and quantified by GCMS, and the resulting proportions are displayed in Fig. 5 (the detailed values are reported in Table S4). Here again, as opposed to *E. coli*, the FA profile is very much perturbed by the addition of PA in the growth medium, at both growth stages. For the most abundant species, the proportion of branched C17 FAs is more altered than the branched C15 FAs, especially in the mid-log phase. As expected, the proportion of PA detected in *B. subtilis* membrane increases with increasing concentration of exogenous PA-d_{31}, at the expense of all other FAs. Concomitantly, deuterium labeling increases, reaching over 40% labeling at 50 μM PA-d_{31}, then leveling over 70% above 100 μM PA-d_{31}. We note the presence of a very small amount (less than 1%) of C18:0-d_{31}, an elongation of the exogenous deuterated C16:0-d_{31}. Altogether, these results indicate that to optimize the ^{2}H-labeling protocol of *B. subtilis*, a low concentration of exogenous PA should be used since it will be integrated in the membrane such that it will be detected by SS-NMR, as already observed [6].

Labeling *B. subtilis* membranes with deuterated FAs enables their *in vivo* study and membrane lipid order assessment by monitoring the M_2 of ^{2}H SS-NMR spectra under MAS. Representative spectra are shown in Fig. 6 and extracted M_2 values are reported in Table 2. ^{2}H SS-NMR results are consistent with those of GCMS, *i.e.*, an increase in rigidity is measured as the proportion of PA-d_{31} is added and incorporated in the phospholipids by the bacteria. This increase is moderate for 20 and 50 μM PA-d_{31}, but is very important for concentrations above 100 μM. Finally, the instability in the mid-log phase observed for *E. coli* was not observed in the case of *B. subtilis*.

To summarize our observations for *B. subtilis* labeling, a concentration of 50 μM of exogenous PA-d_{31} micellized in Tween® 20 should be employed, and bacteria collected at the early stationary phase for *in vivo* ^{2}H SS-NMR analysis. This ensures that *ca.* 40% of FA chains are labeled while branched FAs are reduced by a factor of two approximately. The membrane lipid order can thus be assessed by *in vivo* ^{2}H SS-NMR while retaining a fluidity close to the native one. In such conditions, the headgroup profile of *B. subtilis* is slightly modified, with a doubling of CL at the expense of PG. Unfortunately, the strong reduction of branched FAs is the price to pay, in order to be able to probe the bacterial membrane lipid order by ^{2}H SS-NMR. Since SS-NMR often *compares* different growth conditions, one can expect that even though the starting point has deviated from the native condition, the comparisons still stand. In the case of *B. subtilis*, we are exploring other labeling strategies in order to circumvent these obstacles.

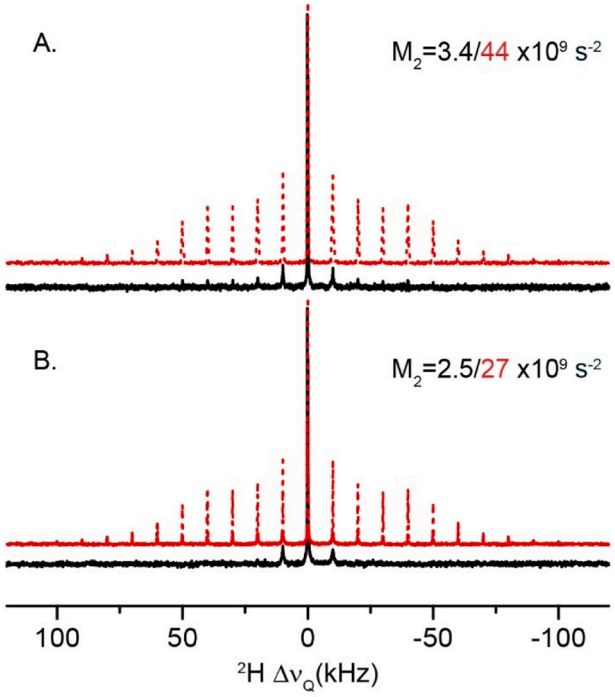

Fig. 6. ^{2}H SS-NMR spectra of *B. subtilis* spun at 10 kHz and 37 °C. Bacteria were grown with either 50 μM (black) or 190 μM (dotted red) of PA-d_{31} and collected at the (A) mid-log or (B) early stationary stages. The resulting M_2 values for all labeling conditions are reported in Table 2. All spectra were normalized with respect to the first spinning sideband to better highlight the sideband intensity distribution. Note that the spectra are zoomed in order to show the difference in sideband intensities, the central peak is thus truncated.

4. Summary and conclusions

In vivo SS-NMR has only recently been applied to bacteria; the approach and the growth conditions are therefore still being optimized. The work presented here is a big step forward as we optimized both the concentration of exogenous labeled PA to be used and the bacterial harvest time to ensure an appropriate labeling yield with minimal perturbation of the native membrane lipid profile. This was facilitated by the fast protocol that we have developed to quantify and characterize bacterial membrane lipids at each step of the optimization process. In addition to GCMS, this protocol makes use of ^{31}P solution NMR, which has allowed confirming the nature of the fourth phospholipid in *B. subtilis* as lysyl-phosphatidylglycerol.

This protocol was developed and optimized for the *in vivo* study of bacteria by SS-NMR, where phospholipids are usually labeled with deuterated FAs. In the case of other labeling schemes, with nuclei such as ^{13}C or ^{19}F, the lipid analysis pipeline proposed here, *i.e.*, solution ^{31}P NMR followed by GCMS, could also be used to characterize the membrane lipid composition. Finally, since phospholipids are abundant in many eukaryotic membranes, this protocol could also be adapted to a variety of cells.

Studying bacteria at various growth phases has shown that the lipid composition of *E. coli* was more stable than that of *B. subtilis*. More importantly, when bacteria are labeled with exogenous deuterated FAs, both their lipid headgroups and FA profiles are perturbed, especially at the mid-log stage. Our protocol has confirmed the necessity to combine PA and OA for *E. coli*, and shown that a concentration of exogenous PA-d_{31} lower than the one used in previous work can be employed. New labeling protocols are suggested: 100 μM of total exogenous PA and OA for *E. coli*, and 50 μM of exogenous PA for *B. subtilis*, both collected at the early stationary phase.

Funding

This work was supported by the Natural Sciences and Engineering Research Council (NSERC) of Canada (grant RGPIN-2018-06200 to I.M.) and the Centre National de la Recherche Scientifique (UMR 7203 to D.E. W.).

CRediT authorship contribution statement

Conceptualization, A.A.A, D.E.W., and I.M.; methodology, data collection and initial analysis, F.L., M.M., P.L., J.-P.B., and L.C.; additional analysis, A.A.A, D.E.W., and I.M.; writing—original draft preparation, D.E.W.; writing—review and editing, F.L., M.M., P.L., J.-P.B., L. C., A.A.A, D.E.W., and I.M.; supervision and funding acquisition, D.E.W. and I.M. All authors have read and agreed to the published version of the manuscript.

Declaration of competing interest

The authors declare that they have no known competing financial interests or personal relationships that could have appeared to influence the work reported in this paper.

Data availability

Data will be made available on request.

Acknowledgments

The authors would like to thank Isabelle Rheault and Galyna Shul for technical assistance. J.-P.B. would like to thank the Natural Sciences and Engineering Research Council (NSERC) of Canada, for the award of a graduate scholarship. I.M. is a member of Ressources Aquatiques Québec (RAQ) and PROTEO research networks.

Appendix A. Supplementary data

Supplementary Materials: The following are available online. Fig. S1: additional ^{31}P solution NMR spectra; Fig. S2: phospholipids cited in this work; Fig. S3: fatty acids cited in this work; Fig. S4: additional ^{2}H solid-state NMR spectra; Tables S1 and S2: ^{31}P solution NMR chemical shifts; Table S3: fatty acid profile of *E. coli*; Table S4: fatty acid profile of *B. subtilis*. Supplementary data to this article can be found online at https://doi.org/10.1016/j.bbamem.2021.183819.

References

[1] J.H. Davis, C.P. Nichol, G. Weeks, M. Bloom, Study of the cytoplasmic and outer membranes of Escherichia coli by deuterium magnetic resonance, Biochemistry 18 (1979) 2103–2112.
[2] J. Pius, M.R. Morrow, V. Booth, 2H solid-state NMR investigation of whole Escherichia coli interacting with antimicrobial peptide MSI-78, Biochemistry 51 (2012) 118–125.
[3] C. Tardy-Laporte, A.A. Arnold, B. Génard, R. Gastineau, M. Morançais, J.-L. Mouget, R. Tremblay, I. Marcotte, A 2H solid-state NMR study of effect of antimicrobials on intact Escherichia coli without mutating, Biochim. Biophys. Acta 1828 (2013) 614–622.
[4] X.L. Warnet, A.A. Arnold, I. Marcotte, D.E. Warschawski, In cell solid-state NMR: an emerging technique for the study of biological membranes, Biophys. J. 109 (2015) 2461–2466.
[5] X.L. Warnet, M. Laadhari, A.A. Arnold, I. Marcotte, D.E. Warschawski, A 2H magic-angle spinning solid-state NMR characterisation of lipid membranes in intact bacteria, Biochim. Biophys. Acta 1858 (2016) 146–152.
[6] M. Laadhari, A.A. Arnold, A.E. Gravel, F. Separovic, I. Marcotte, Interaction of the antimicrobial peptides caerin 1.1 and aurein 1.2 with intact bacteria by 2H solid-state NMR, Biochim. Biophys. Acta 1858 (2016) 2959–2964.
[7] V. Booth, D.E. Warschawski, N.P. Santisteban, M. Laadhari, I. Marcotte, Recent progress on the application of 2H solid-state NMR to probe the interaction of antimicrobial peptides with intact bacteria, Biochim. Biophys. Acta 1865 (2017) 1500–1511.
[8] Z. Bouhlel, A.A. Arnold, D.E. Warschawski, K. Lemarchand, R. Tremblay, I. Marcotte, Labelling strategy and membrane characterization of marine bacteria Vibrio splendidus by in vivo 2H NMR, Biochim. Biophys. Acta 1861 (2019) 871–878.
[9] N.P. Santisteban, M.R. Morrow, V. Booth, Effect of AMPs MSI-78 and BP100 on the lipid acyl chains of 2H-labeled intact gram positive bacteria, Biochim. Biophys. Acta 1862 (2020), 183199.
[10] Z. Bouhlel, A.A. Arnold, J.S. Deschênes, J.L. Mouget, D.E. Warschawski, R. Tremblay, I. Marcotte, Investigating the action of the microalgal pigment marennine on Vibrio splendidus by in vivo 2H and 31P solid-state NMR, Biochim. Biophys. Acta 1863 (2021), 183642.
[11] F. Ianzini, L. Guidoni, G. Simone, V. Viti, M.B. Yatvin, Effects of decreased pH on membrane structural organization of Escherichia coli grown in different fatty acid-supplemented media: a 31P NMR study, Arch. Biochem. Biophys. 278 (1990) 1–10.
[12] A.G. Rietveld, J.A. Killian, W. Dowhan, B. de Kruijff, Polymorphic regulation of membrane phospholipid composition in Escherichia coli, J. Biol. Chem. 268 (1993) 12427–12433.
[13] S. Morein, A. Andersson, L. Rilfors, G. Lindblom, Wild-type Escherichia coli cells regulate the membrane lipid composition in a "window" between gel and non-lamellar structures, J. Biol. Chem. 271 (1996) 6801–6809.
[14] L.E. Cybulski, D. Albanesi, M.C. Mansilla, S. Altabe, P.S. Aguilar, D. de Mendoza, Mechanism of membrane fluidity optimization: isothermal control of the Bacillus subtilis acyl-lipid desaturase, Mol. Microbiol. 45 (2002) 1379–1388.
[15] T. Romantsov, Z. Guan, J.M. Wood, Cardiolipin and the osmotic stress responses of bacteria, Biochim. Biophys. Acta 1788 (2009) 2092–2100.
[16] X. Gao, W. Liu, J. Mei, J. Xie, Quantitative analysis of cold stress inducing lipidomic changes in shewanella putrefaciens using UHPLC-ESI-MS/MS, Molecules 24 (2019) 4609.
[17] J.D. Nickels, S. Poudel, S. Chatterjee, A. Farmer, D. Cordner, S.R. Campagna, R. J. Giannone, R.L. Hettich, D.A.A. Myles, R.F. Standaert, J. Katsaras, J.G. Elkins, Impact of fatty-acid labeling of Bacillus subtilis membranes on the cellular lipidome and proteome, Front. Microbiol. 11 (2020) 914.
[18] T.Z. Lee, V. Hofferek, M.A. Sani, F. Separovic, G.E. Reid, M.I. Aguilar, The impact of antibacterial peptides on bacterial lipid membranes depends on stage of growth, Faraday Discuss (2021), https://doi.org/10.1039/D0FD00052C. Advance Article.
[19] T.G. Meikle, K. Huynh, C. Giles, P.J. Meikle, Clinical lipidomics: realizing the potential of lipid profiling, J. Lipid Res. 62 (2021), 100127.
[20] R.D. Mavis, P.R. Vagelos, The effect of phospholipid fatty acid composition on membranous enzymes in Escherichia coli, J. Biol. Chem. 247 (1972) 652–659.
[21] A.A. Sey, T.H. Pham, V. Kavanagh, S. Kaur, M. Cheema, L. Galagedara, R. Thomas, Canola produced under boreal climatic conditions in Newfoundland and Labrador have a unique lipid composition and expeller press extraction retained the composition for commercial use, J. Adv. Res. 24 (2020) 423–434.
[22] C.S. Lopez, A.F. Alice, H. Heras, E.A. Rivas, C. Sanchez-Rivas, Role of anionic phospholipids in the adaptation of Bacillus subtilis to high salinity, Microbiology 152 (2006) 605–616.

[23] B. Fuchs, R. Suss, K. Teuber, M. Eibisch, J. Schiller, Lipid analysis by thin-layer chromatography—a review of the current state, J. Chromatogr. A 1218 (2011) 2754–2774.
[24] B.K. Tan, M. Bogdanov, J. Zhao, W. Dowhan, C.R.H. Raetz, Z. Guan, Discovery of a cardiolipin synthase utilizing phosphatidylethanolamine and phosphatidylglycerol as substrates, Proc. Natl. Acad. Sci. U. S. A. 109 (2012) 16504–16509.
[25] P. Uttlová, D. Pinkas, O. Bechyňková, R. Fišer, J. Svobodová, G. Seydlová, Bacillus subtilis alters the proportion of major membrane phospholipids in response to surfactin exposure, Biochim. Biophys. Acta 1858 (2016) 2965–2971.
[26] A. Nahar, A.L. Baker, D.S. Nichols, J.P. Bowman, M.L. Britz, Application of thin-layer chromatography-flame ionization detection (TLC-FID) to Total lipid quantitation in mycolic-acid synthesizing Rhodococcus and Williamsia species, Int. J. Mol. Sci. 21 (2020) 1670.
[27] P. Meneses, T. Glonek, High resolution 31P NMR of extracted phospholipids, J. Lipid Res. 29 (1988) 679–689.
[28] N. Culeddu, M. Bosco, R. Toffanin, P. Pollesello, 31P NMR analysis of phospholipids in crude extracts from different sources: improved efficiency of the solvent system, Magn. Reson. Chem. 36 (1998) 907–912.
[29] A. Flieger, S. Gongab, M. Faigle, H.A. Mayer, U. Kehrer, J. Mussotter, P. Bartmann, B. Neumeister, Phospholipase a secreted by legionella pneumophila destroys alveolar surfactant phospholipids, FEMS Microbiol. Lett. 188 (2000) 129–133.
[30] S. Murgia, S. Mele, M. Monduzzi, Quantitative characterization of phospholipids in Milk fat via 31 P NMR using a monophasic solvent mixture, Lipids 38 (2003) 585–591.
[31] R. Estrada, N. Stolowich, M.C. Yappert, Influence of temperature on 31P NMR chemical shifts of phospholipids and their metabolites I. In chloroform-methanol-water, Anal. Biochem. 380 (2008) 41–50.
[32] S. Kaffarnik, I. Ehlers, G. Gröbner, J. Schleucher, W. Vetter, Two-dimensional 31P,1H NMR spectroscopic profiling of phospholipids in cheese and fish, J. Agric. Food Chem. 61 (2013) 7061–7069.
[33] J. Li, T. Vosegaard, Z. Guo, Applications of nuclear magnetic resonance in lipid analyses: an emerging powerful tool for lipidomics studies, Prog. Lipid Res. 68 (2017) 37–56.
[34] R.P. Rehal, H. Marbach, A.T.M. Hubbard, A.A. Sacranie, F. Sebastiani, G. Fragneto, R.D. Harvey, The influence of mild acidity on lysyl-phosphatidylglycerol biosynthesis and lipid membrane physico-chemical properties in methicillin-resistant staphylococcus aureus, Chem. Phys. Lipids 206 (2017) 60–70.
[35] S. Furse, M. Jakubec, F. Rise, H.E. Williams, C.E.D. Rees, Ø. Halskau, Evidence that Listeria innocua modulates its membrane's stored curvature elastic stress, but not fluidity, through the cell cycle, Sci. Rep. 7 (2017) 8012.
[36] J. Schiller, M. Müller, B. Fuchs, K. Arnold, D. Huster, 31P NMR spectroscopy of phospholipids: from micelles to membranes, Curr. Anal. Chem. 3 (2007) 283–301.
[37] A. Singh, A. MacKenzie, G. Girnun, M. Del Poeta, Analysis of sphingolipids, sterols, and phospholipids in human pathogenic cryptococcus strains, J. Lipid Res. 58 (2017) 2017–2036.
[38] D. Oursel, C. Loutelier-Bourhis, N. Orange, S. Chevalier, V. Norris, C.M. Lange, Lipid composition of membranes of Escherichia coli by liquid chromatography/tandem mass spectrometry using negative electrospray ionization, Rapid Commun. Mass Spectrom. 21 (2007) 1721–1728.
[39] P. Bernat, K. Paraszkiewicz, P. Siewiera, M. Moryl, G. Płaza, J. Chojniak, Lipid composition in a strain of Bacillus subtilis, a producer of iturin A lipopeptides that are active against uropathogenic bacteria, World J. Microbiol. Biotechnol. 32 (2016) 157.
[40] T.H. Pham, M. Zaeem, T.A. Fillier, M. Nadeem, N.P. Vidal, C. Manful, S. Cheema, M. Cheema, R.H. Thomas, Targeting modified lipids during routine lipidomics analysis using HILIC and C30 reverse phase liquid chromatography coupled to mass spectrometry, Sci. Rep. 9 (2019) 5048.
[41] K. Kanonenberg, J. Royes, A. Kedrov, G. Poschmann, F. Angius, A. Solgadi, O. Spitz, D. Kleinschrodt, K. Stühler, B. Miroux, L. Schmitt, Shaping the lipid composition of bacterial membranes for membrane protein production, Microb. Cell Factories 18 (2019) 131–142.
[42] R. Dazzoni, C. Bure, E. Morvan, A. Grelard, C. Gounou, J.-M. Schmitter, A. Loquet, B. Larijani, E.J. Dufourc, Tandem NMR and mass spectrometry analysis of human nuclear membrane lipids, Anal. Chem. 92 (2020) 6858–6868.
[43] Z. DeMars, V.K. Singh, J.L. Bose, Exogenous fatty acids remodel Staphylococcus aureus lipid composition through fatty acid kinase, J. Bacteriol. 202 (2020) e00128-20.
[44] J. Folch, M. Lees, G.H.A. Sloane Stanley, Simple method for the isolation and purification of total lipides from animal tissues, J. Biol. Chem. 226 (1957) 497–509.
[45] R.K. Harris, E.D. Becker, S.M. Cabral de Menezes, R. Goodfellow, P. Granger, NMR nomenclature. Nuclear spin properties and conventions for chemical shifts, Pure Appl. Chem. 73 (2001) 1795–1818.

Supplementary Materials

Growth-phase dependence of bacterial membrane lipid profile and labeling for in-cell solid-state NMR applications

Florent Laydevant,[a] Mahsa Mahabadi,[a] Pierre Llido,[a] Jean-Philippe Bourgouin,[a] Laurence Caron,[a] Alexandre A. Arnold,[a] Isabelle Marcotte[a] and Dror E. Warschawski[a,b*]*

[a] Departement of chemistry, Université du Québec à Montréal, C.P. 8888, Succursale Centre-Ville, Montreal H3C 3P8, Canada

[b] Laboratoire des Biomolécules, LBM, CNRS UMR 7203, Sorbonne Université, École normale supérieure, PSL University, 75005 Paris, France

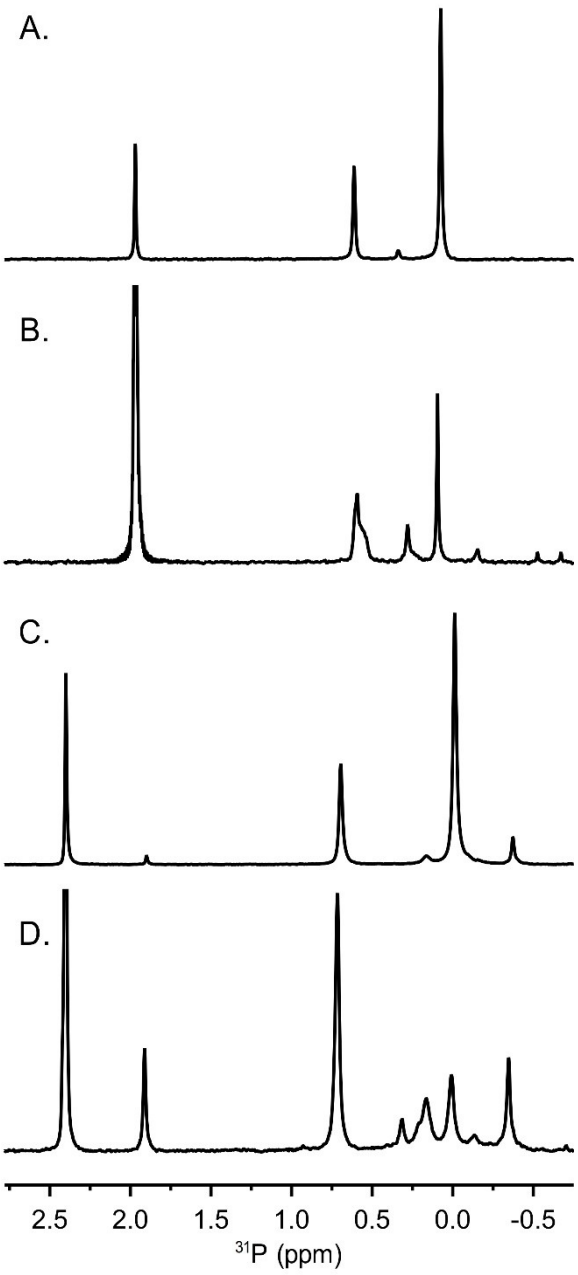

Figure S1. ^{31}P solution NMR spectra of extracted bacterial lipids in organic solvent solutions: (A) *E. coli* in the biphasic solution; (B) *B. subtilis* in the biphasic solution; (C) *E. coli* in the *CUBO* solution; (D) *B. subtilis* in the *CUBO* solution (see Material and Methods). Note that our internal reference is TMP at 2.01 ppm in the biphasic solution, and at 2.42 ppm in the *CUBO* solution.

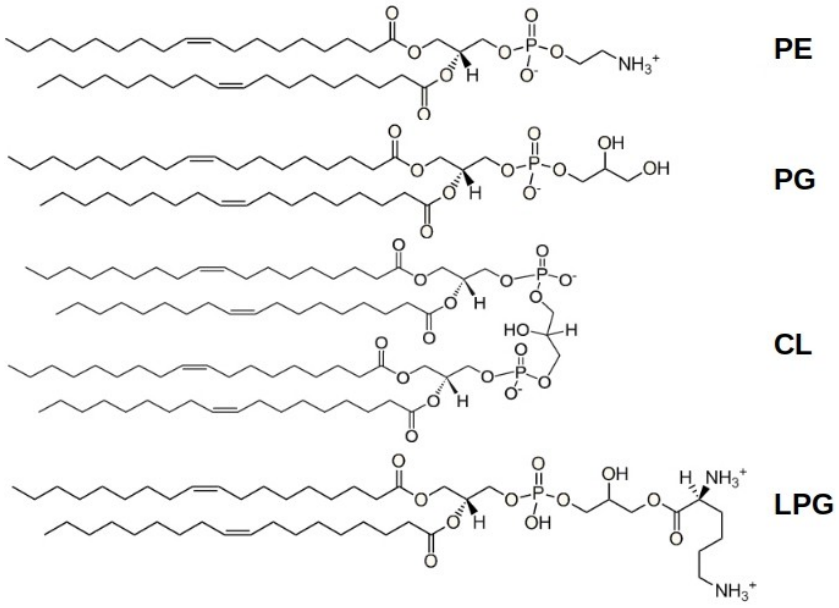

Figure S2. Phospholipids cited in this work (fatty acids represented here are C18:1).

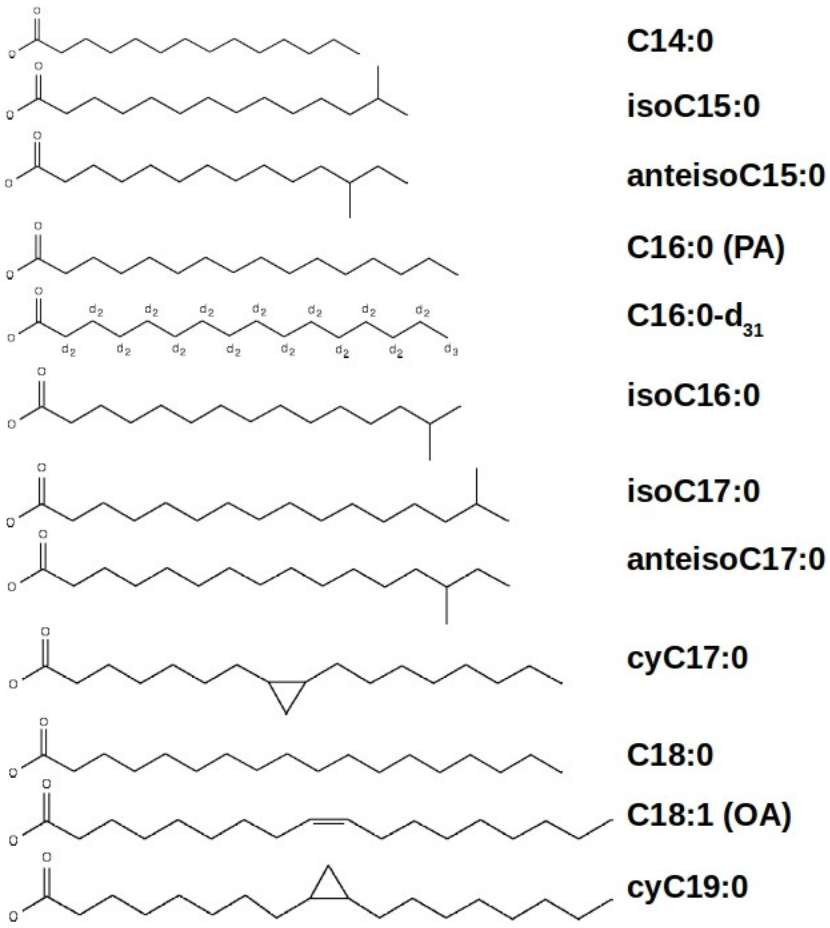

Figure S3. Fatty acids cited in this work.

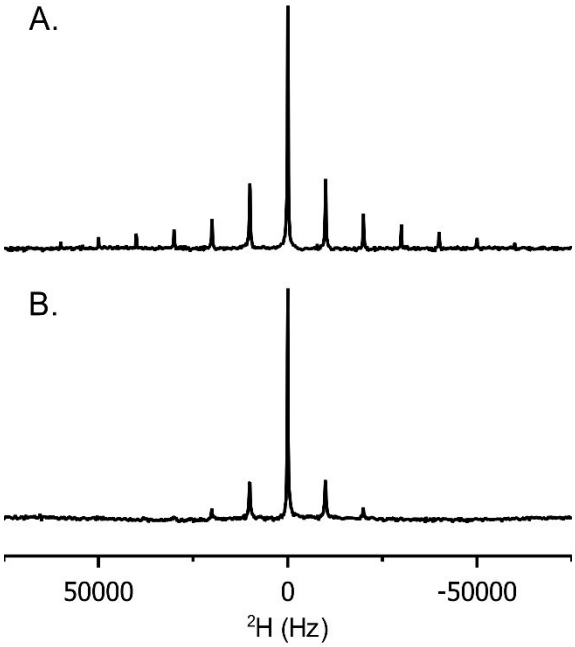

Figure S4. ^{2}H solid-state NMR spectra of (A) an *E. coli* pellet grown with 190 µM of PA-d_{31} and OA, and collected at mid-log, spinning at 10 kHz and 37°C; (B) the same pellet, two hours later.

Table S1. ^{31}P solution NMR chemical shifts of various compounds in two organic solvent solutions at 25°C (see Material and Methods).

Compounds	In biphasic solution	In *CUBO* solution
TMP	2.01 ppm	2.42 ppm and 1.92 ppm
POPG	0.63 ppm	0.76 ppm
POPA	0.50 ppm	4.89 ppm
TMCL	0.37 ppm	0.29 ppm
POPE	0.08 ppm	0.03 ppm and -0.33 ppm
Egg SM	-0.04 ppm	0.34 ppm
POPS	-0.07 ppm	0.06 ppm and -0.24 ppm
POPC	-0.81 ppm	-0.48 ppm

Table S2. ^{31}P solution NMR chemical shifts of bacterial lipids in two organic solvent solutions at 25°C, with standard deviation indicated (see Material and Methods).

Lipid	*E. coli* in biphasic solution	*E. coli* in *CUBO* solution	*B. subtilis* in biphasic solution	*B. subtilis* in *CUBO* solution
PG	0.65 ppm (0.02)	0.77 ppm (0.03)	0.65 ppm (0.02)	0.78 ppm (0.03)
CL	0.38 ppm (0.03)	0.25 ppm (0.04)	0.37 ppm (0.05)	0.25 ppm (0.04)
PE	0.11 ppm (0.04)	-0.05 ppm (0.03) and -0.31 ppm (0.05)	0.14 ppm (0.04)	0.06 ppm (0.03) and -0.30 ppm (0.05)
Lysyl-PG			-0.11 ppm (0.04)	0.38 ppm (0.03)
unknown			-0.48 ppm (0.03)	-0.08 ppm (0.03)

Table S3. Fatty acid profile of *E. coli* grown with various concentrations of PA-d_{31} and OA, at different growth stages, as determined by GCMS, with standard deviation indicated. Values for C16:0-d_{31} indicate the percentage of deuteration of palmitic acid. Deuterated C14:0 and other minor fatty acids have been detected but are not indicated here for simplification.

	0 μM		**50 μM**		**100 μM**		**190 μM**	
	Mid-log	**Early stationary**	**Mid-log**	**Early stationary**	**Mid-log**	**Early stationary**	**Mid-log**	**Early stationary**
C14:0	3.3% (0.2)	2.1% (1.5)	1.5% (0.1)	2.1% (0.1)	1.3% (0.2)	3.2% (0.1)	1.5% (0.2)	2.0% (0.1)
C16:0 **(C16:0-d_{31})**	38.6% (4.0)	45.0% (3.6)	43.9% (4.0) (48%)	36.9% (4.1) (40%)	44.3% (3.6) (56%)	39.3% (0.1) (54%)	48.1% (6.3) (56%)	37.8% (1.1) (54%)
cyC17:0	17.6% (0.4)	24.3% (3.9)	10.7% (3.5)	16.0% (2.1)	9.1% (2.6)	14.1% (0.1)	7.9% (1.9)	16.6% (1.1)
C18:0	0.8% (0.5)	1.6% (1.2)	1.1% (0.7)	1.5% (1.1)	1.0% (0.6)	0.9% (0.1)	0.8% (0.5)	0.4% (0.1)
C18:1	30.9% (0.8)	4.7% (3.0)	40.7% (1.1)	33.6% (4.1)	42.2% (2.2)	28.3% (3.1)	40.4% (4.9)	29.8% (2.1)
cyC19:0	6.3% (0.5)	20.5% (2.3)	2.2% (0.7)	9.7% (3.1)	1.9% (1.1)	13.8% (2.1)	1.4% (0.3)	13.3% (2.1)
Total cyclopropane	24%	45%	13%	26%	11%	28%	9%	30%
Total unsaturated	31%	5%	41%	34%	42%	28%	40%	30%
Total saturated	45%	50%	46%	40%	47%	44%	51%	40%

Table S4. Fatty acid profile of *B. subtilis* grown with various concentrations of PA-d_{31}, at different growth stages, as determined by GCMS, with standard deviation indicated. Values for C16:0-d_{31} indicate the percentage of deuteration of palmitic acid. Deuterated C18:0 and other minor fatty acids have been detected but are not indicated here, for simplification.

	0 µM		**20 µM**		**50 µM**		**100 µM**		**190 µM**	
	Mid-log	**Early stationary**	**Mid-log**	**Early stationary**	**Mid-log**	**Early stationary**	**Mid-log**	**Early stationary**	**Mid-log**	**Early stationary**
isoC15:0	10.9% (0.5)	18.0% (0.1)	8.7% (0.9)	9.0% (0.4)	2.7% (0.6)	5.3% (1.5)	3.3% (1.2)	2.3% (0.1)	0.5% (0.1)	2.9% (0.7)
anteisoC15:0	26.9% (1.4)	45.6% (0.7)	32.0% (3.0)	30.0% (0.9)	15.3% (3.8)	21.1% (1.9)	12.8% (4.6)	8.8% (0.1)	2.0% (0.7)	10.9% (3.5)
isoC16:0	4.4% (3.3)	3.7% (0.2)	5,0% (0.7)	5.3% (0.3)	1.1% (0.8)	3.0% (0.4)	1.5% (0.3)	1.0% (0.2)	0.2% (0.1)	1.3% (0.3)
C16:0 **(C16:0-d_{31})**	8.4% (5.9)	5.4% (1.1)	29.7% (8.7) (70%)	24.2% (4.1) (48%)	70.5% (16.4) (81%)	50.3% (3.6) (75%)	71.9% (9.5) (94%)	79.2% (0.6) (91%)	95.2% (1.1) (98%)	75.1% (8.9) (93%)
isoC17:0	19.0% (3.4)	10.8% (0.1)	8.9% (1.3)	11.3% (0.3)	3.2% (1.8)	6.4% (1.7)	3.4% (1.3)	2.6% (0.2)	0.4% (0.1)	3.2% (1.1)
anteisoC17:0	29.7% (7.0)	16.4% (0.1)	13.2% (1.6)	12.9% (0.4)	6.2% (1.2)	8.5% (1.7)	5.8% (1.8)	3.8% (0.1)	1.3% (0.2)	4.7% (1.4)
C18:0	0.0% (0.0)	1.2% (0.0)	2.8% (0.3)	7.3% (0.6)	1.0% (0.7)	5.4% (2.7)	1.3% (0.1)	2.2% (0.3)	0.6% (0.2)	2.0% (0.3)
Total branched	92%	94%	68%	69%	29%	45%	28%	19%	4%	23%
Total non branched	8%	6%	32%	31%	71%	55%	72%	82%	96%	77%